Journal of Pharmaceutical and Biomedical Analysis 52 (2010) 345–354

Contents lists available at ScienceDirect

Journal of Pharmaceutical and Biomedical Analysis

journal homepage: www.elsevier.com/locate/jpba

LC and LC–MS/TOF studies on stress degradation behaviour of candesartan cilexetil

Surbhi Mehta, Ravi P. Shah, Rajkamal Priyadarshi, Saranjit Singh*

Department of Pharmaceutical Analysis, National Institute of Pharmaceutical Education and Research (NIPER), Sector 67, S.A.S. Nagar 160 062, Punjab, India

ARTICLE INFO

Article history:
Received 2 April 2009
Received in revised form 7 May 2009
Accepted 7 May 2009
Available online 15 May 2009

Keywords:
Candesartan cilexetil
Stress degradation study
LC–MS/TOF
MS^n
Degradation products
Characterization

ABSTRACT

Stress degradation studies were conducted on candesartan cilexetil under the ICH prescribed conditions of hydrolysis (acidic, basic and neutral), photolysis, oxidation and thermal stress. Maximum degradation was observed on hydrolysis, especially in the neutral condition. The drug was also degraded significantly under photolytic conditions. However, it was stable to oxidative and thermal stress. A total of eight degradation products were formed, the separation of which was successfully achieved on a C-18 column employing a gradient method. In order to characterize each degradation product, a complete mass fragmentation pathway of the drug was initially established with the help of MS^n and MS/TOF accurate mass studies. Subsequently, degradation products were also subjected to LC–MS/TOF investigations, which resulted in their fragmentation pattern and also accurate masses. The latter helped in the elucidation of the structure of all the degradation products, which was achieved through comparison of their fragmentation pattern with that of the drug. The major product was isolated and its structure was confirmed through NMR studies. On the whole, a more comprehensive fragmentation behaviour and degradation profile of the drug was established than reported in the literature.

© 2009 Elsevier B.V. All rights reserved.

1. Introduction

Candesartan cilexetil belongs to the class of angiotensin receptor antagonists and acts by binding selectively and non-competitively to angiotensin II receptor type 1, thus preventing actions of angiotensin II. The drug finds most significant clinical use in the treatment of hypertension of all grades. Chemically, candesartan cilexetil is an ester prodrug of its active metabolite candesartan, to which it owes its therapeutic effect [1].

The chemical stability of candesartan cilexetil has been studied in plasma and bioanalytical samples [2]. Under these conditions, the drug was found to be susceptible to hydrolysis, resulting in the removal of cilexetil moiety. In another study involving development of a stability-indicating analytical method [3], candesartan cilexetil was observed to be converted to four degradation products (DPs), whose structures are shown in Fig. 1. As evident, the reported products 3 and 4 were ethylated in the tetrazole moiety at positions *N*1 and *N*4, respectively. The given structures of these DPs were not convincing, considering that tetrazole ring has a symmetry axis and hence the two are stereochemically identical. This conjecture led us to re-look into the degradation profile of candesartan cilexetil.

The drug was exposed to ICH prescribed conditions of hydrolytic, oxidative, photolytic and thermal stress. The stressed samples were subjected to HPLC, and the components were separated on a reversed-phase column. A total of eight products were formed under different conditions, which were characterized by determination of their accurate mass and comparison of MS fragmentation behaviour with that of the drug. A major product was also isolated and its structure was confirmed through NMR studies. The details are provided in this communication.

2. Experimental

2.1. Drug and reagents

Candesartan cilexetil was obtained as a gratis sample from Ranbaxy Research Laboratories (Gurgaon, India). It was used without further purification. Analytical reagent (AR) grade sodium hydroxide was purchased from Ranbaxy Laboratories (SAS Nagar, India), hydrochloric acid from LOBA Chemie Pvt. Ltd. (Mumbai, India) and hydrogen peroxide from s.d. fine-chem Ltd. (Boisar, India). Buffer salts and all other chemicals were bought from local suppliers. HPLC grade acetonitrile (ACN) was procured from J.T. Baker (Mexico City, Mexico). Ultra pure water obtained from ELGA water purification unit (Wycombe, Bucks, England) was used throughout the studies.

2.2. Apparatus and equipment

Precision water baths equipped with MV controller (Julabo, Seelbach, Germany) were used for solution degradation studies.

* Corresponding author. Tel.: +91 172 2214682; fax: +91 172 2214692.
E-mail address: ssingh@niper.ac.in (S. Singh).

0731-7085/$ – see front matter © 2009 Elsevier B.V. All rights reserved.
doi:10.1016/j.jpba.2009.05.006

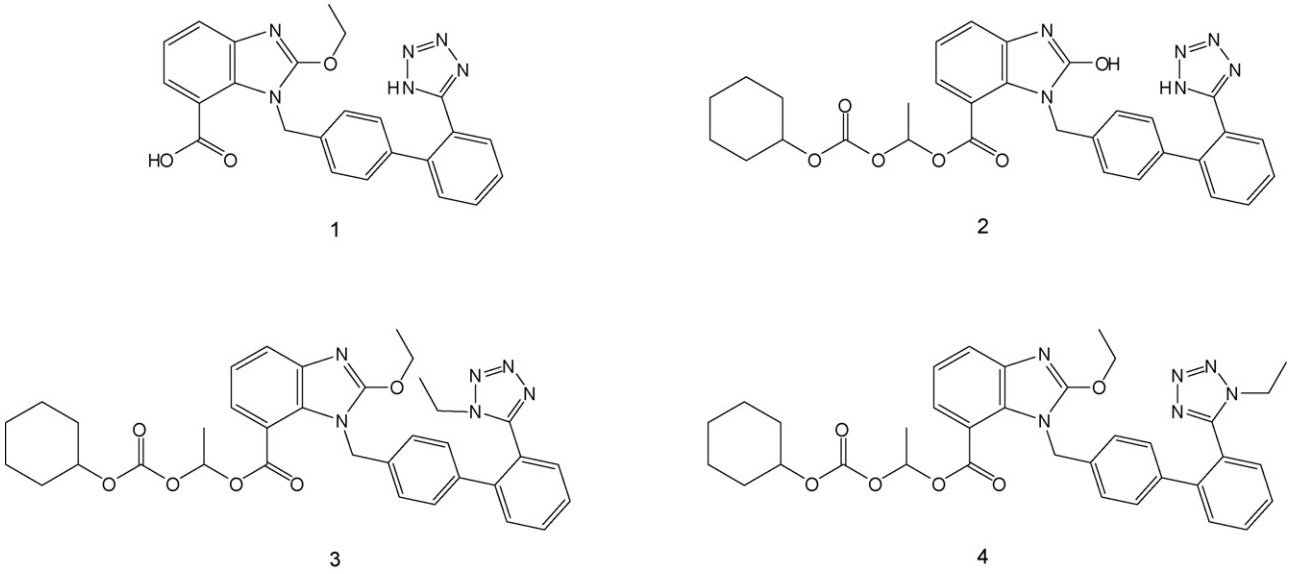

Fig. 1. Structures of the reported degradation products.

A Dri-Bath (Thermolyne, IA, USA) was used for solid state thermal stress studies. Accelerated stability studies were carried out in humidity (KBF720, WTC Binder, Tuttlingen, Germany) and photostability (KBWF 240, WTC Binder) chambers, both set at 40 ± 1 °C/75 ± 3% RH. The photostability chamber was equipped with an illumination bank on inside top, consisting of a combination of two UV (OSRAM L18 W/73) and four white fluorescent (PHILIPS TRULITE 18W/86) lamps, in accordance with Option 2 of the ICH guideline Q1B [4]. Both fluorescent and UV lamps were put on simultaneously. The samples were placed at a distance of 9 inches from the light bank. A calibrated lux meter (model ELM 201, Escorp, New Delhi, India) and a calibrated UV radiometer (model 206, PRC Krochmann GmbH, Berlin, Germany) were used to measure visible illumination and UV energy, respectively. The HPLC system consisted of an on-line degasser (DGU-14A), low-pressure gradient flow control valve (FCV-10ALVP), solvent delivery module (LC-10ATVP), auto-injector (SIL-10ADVP), column oven (CTO-10ASVP), UV–visible dual-wavelength detector (SPD-10AVP), photo-diode array (PDA) detector (SPD-M10AVP), system controller (SCL-10AVP) and a computer system loaded with CLASS VP software (all from Shimadzu, Kyoto, Japan). Multi-stage MS (MS^n) studies were carried out on LTQ XL MS 2.5.0 (Thermo, San Jose, USA). The same was controlled by Xcalibur (version 2.0.7 SP1) software. LC–MS/TOF studies were carried out on a system, in which LC part consisted of 1100 series HPLC from Agilent Technologies (Waldbronn, Germany). The MS part consisted of MicrOTOF-Q spectrometer (from Bruker Daltonik, Bremen, Germany), which was operated using Hyphenation Star (version 3.1) and MicrOTOF Control (version 2.0) software. The calibration solution used was ES Tuning Mix solution (Agilent Technologies, USA), diluted to a suitable concentration with a mixture of ACN–water (95:5%, v/v). The system was calibrated prior to analysis of the test samples. All masses were corrected by use of internal reference ions of *m/z* 322.0481 ($C_6H_{19}O_6N_3P_3$), 622.0290 ($C_{12}H_{19}O_6N_3P_3F_{12}$), and 922.0098 ($C_{18}H_{19}O_6N_3P_3F_{24}$). In all the studies, the separations were achieved on a Luna C-18 (150 mm × 4.6 mm i.d., particle size 5 μm) column (Phenomenex, CA, USA). The ^{1}H NMR and DEPT 135 investigations were carried out on an Avance III 400 NMR spectrometer (Bruker, Switzerland). The same was controlled by Topspin (version 2.1) software. The FT-IR spectrum was recorded on Spectrum 1 FT-IR spectrometer (Perkin-Elmer, CT, USA), monitored by Spectrum (version 3.02) software in the detection range 400 to 4000 cm^{-1} with 4 cm^{-1} resolution.

2.3. Stress studies

The stress studies were carried out under the conditions of hydrolysis, photolysis, oxidation and dry heat, as defined in the ICH guideline Q1A (R2) [5]. Acidic and alkaline hydrolysis were carried out in 0.1N HCl and 0.1N NaOH, respectively, whereas neutral hydrolysis was performed in water. All the hydrolytic studies were conducted at 80 °C. The oxidative study was carried out in 30% H_2O_2 at room temperature for 2 days. The photostability testing in solution was carried out by exposing the solutions of drug in 0.01N HCl, 0.01N NaOH and water to light for 8 days. For solid state photolytic studies, a 1 mm thin layer of drug was exposed to light for a period of 10 days. For thermal stress testing, the drug was sealed in glass vials and placed in a thermostatic block at 50 °C for 21 days. The optimized stressed conditions are enlisted in Table 1.

The stressors, choice of their concentration and preparation of samples were based on a previous publication [6]. As the drug was insoluble in water, the drug stock was prepared in acetonitrile at a concentration of 2 mg/ml. Before the study, the stock was diluted in 50:50 ratio with the stressor (e.g., HCl, NaOH, water, etc.).

2.4. Preparation of samples for HPLC analyses

Samples were withdrawn at suitable time intervals and diluted four times with H_2O:ACN (50:50, v/v) before injection into HPLC. Also, all the stressed samples were mixed in an equal volume and

Table 1
Stress conditions for optimum degradation.

Stress condition	Concentration of stressor	Exposure condition	Duration
Hydrolysis			
Acid	0.1N HCl		1 h
Neutral	H_2O	80 °C	30 h
Base	0.1N NaOH		1 h
Oxidation	30% H_2O_2	RT	2 d
Photolysis 8500 lx fluorescent and 0.05 W/m² UV light			
Acid	0.01N HCl		8 d
Neutral	H_2O	40 °C	8 d
Base	0.01N NaOH	75%RH	8 d
Solid	–		10 d
Thermal	–	50 °C	21 d

Table 2
Parameters of the developed MS/TOF methods.

	Methods	
	1	2
Objective	Molecular ions of drug/degradation products	Optimum fragmentation
Mode	ESI +ve	ESI +ve
Source		
End plate offset (V)	−500	−500
Capillary (V)	−4500	−4500
Nebulizer (bar)	1.2	1.2
Dry gas (l/min)	6.0	6.0
Dry temperature (°C)	200	200
Transfer		
Funnel 1 RF (Vpp)	150	180
Funnel 2 RF (Vpp)	200	200
ISCID energy (eV)	0.0	2.0
Hexapole RF (Vpp)	320	250
Quadrupole		
Ion energy	5.0	0.0
Low mass (*m*/*z*)	300	250
Collision cell		
Collision energy (eV/z)	22.0	20.0
Transfer time (μs)	55.0	50.0
Collision RF (Vpp)	350	300
Pre-pulse storage (μs)	5.0	8.0
Detector		
Source (V)	−1200	−1200

used for HPLC method development. The injection volume was 6 μl in all the cases.

2.5. HPLC method development and optimization

Various mobile phases, viz., acetonitrile, methanol, potassium dihydrogen orthophosphate buffer and sodium dihydrogen orthophosphate buffer were tried to resolve the degradation products. Also, the proportions of organic mobile phase and buffer, pH and the flow rate were systematically varied to optimize the method. Finally, adequate separation of peaks with good resolution was obtained on a C-18 column employing a mobile phase composed of acetonitrile (A) and potassium dihydrogen orthophosphate buffer (B) (pH 2.8; 0.01 M) in a gradient mode (T_{min}/A:B; T_0/62:38; T_6/30:70; T_{10}/26:74; T_{14}/15:85; T_{16}/10:90; T_{21}/62:38; T_{28}/62:38). The detection wavelength was 254 nm and the flow rate was 1.0 ml/min.

2.6. MS/TOF and MS^n studies on the drug

To establish the fragmentation pathway of the drug, MS/TOF studies were performed in ESI positive mode in the mass range of 50–1500. High purity nitrogen was used as nebulizer as well as auxiliary gas. Mass parameters were optimized, as listed in Table 2. The drug was further subjected to multi-stage mass studies (MS^n) in ESI positive mode. Fragmentation of various precursor ions formed in MS^n studies was achieved at different collision energies.

2.7. LC–MS/TOF studies on degradation products

The drug and the stressed drug samples were subjected to LC–MS/TOF studies using the developed LC method; however, phosphate buffer was replaced by ammonium acetate buffer of same concentration and pH. The identity of each degradation product was established with the help of its LC–MS fragmentation analyses, and experimental accurate *m*/*z* values obtained upon calibration of the system with the Tuning Mix solution.

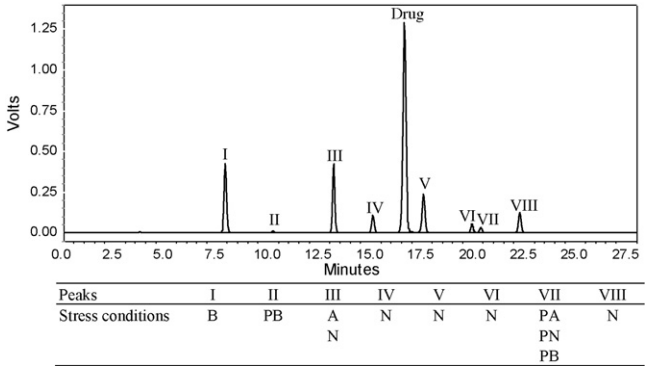

Peaks	I	II	III	IV	V	VI	VII	VIII
Stress conditions	B	PB	A N	N	N	N	PA PN PB	N

Fig. 2. Chromatogram showing separation of degradation products (I–VIII) and drug in the mixture of stressed samples.Key: I–VIII: degradation products; A: acid; B: base; N: neutral; PA: photoacid; PN: photoneutral; PB: photobase.

2.8. IR and NMR studies on isolated degradation product

Degradation product III was isolated and subjected to IR and NMR analyses (^{1}H NMR and DEPT 135) for the confirmation of its structure.

3. Results and discussion

3.1. Degradation behaviour

The drug mainly showed degradation under hydrolytic and photolytic conditions. While five degradation products were formed in water (III, IV, V, VI and VIII), one degradation product each was formed under basic (I) as well as acidic (III) conditions. Under photolytic basic condition, a major degradation product, II was formed, while VII was formed under all photolytic degradation conditions in solution state. Otherwise, the drug was stable to thermal stress, oxidation, and photolysis in solid state. The chromatogram of the mixture of degraded samples is shown in Fig. 2.

3.2. Fragmentation pathway of the drug

A total of 13 fragments were formed on subjecting the drug to MS/TOF. The line spectrum is shown in Fig. 3, where the fragments are labelled from 1 to 13, while the drug is numbered 0. The major fragments of the drug had accurate *m*/*z* values of 441.1705, 423.1590, 395.1501 and 349.1090. Using the data, the best possible molecular formula for each fragment was generated with the help of elemental composition calculator. The same are listed in Table 3. For the elucidation of structures of fragments, multi-stage mass studies (MS^n) were carried out by taking the fragments in a sequential order. In MS^2 studies, M+H = 611 was fragmented into two major fragments

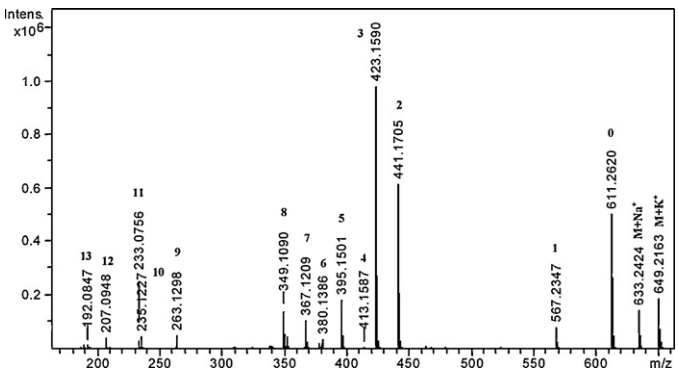

Fig. 3. Line spectrum of the drug obtained in an MS/TOF study.

Table 3
Interpretation of MS/TOF and MS^n data of fragments of the drug.

Peak No.	Experimental mass	Best possible molecular formula	Theoretical mass	Error in ppm	RDB	Possible parent fragment	Difference from parent ion	Possible losses corresponding to difference
0	611.2620	$C_{33}H_{35}N_6O_6$	611.2613	1.1	19.5			
1	567.2347	$C_{31}H_{31}N_6O_5$	567.2350	−0.5	19.5	0	44.0273	N_3H_2 C_2H_4O
2	441.1705	$C_{24}H_{21}N_6O_3$	441.1670	7.9	17.5	0, 1	170.0915, 126.0642	$C_9H_{14}O_3$, $C_7H_{10}O_2$ $C_{12}H_{12}N$, $C_6H_8NO_2$
3	423.1590	$C_{24}H_{19}N_6O_2$	423.1564	6.1	18.5	2	18.0115	H_2O
4	413.1587	$C_{24}H_{21}N_4O_3$	413.1608	−5.1	19.5	2	28.0118	N_2 CH_2N
5	395.1501	$C_{24}H_{19}N_4O_2$	395.1503	−0.5	17.5	3, 4	28.0089, 18.0086	N_2, H_2O CH_2N
6	380.1386	$C_{24}H_{18}N_3O_2$	380.1394	−2.1	17.5	5	15.0115	NH
7	367.1209	$C_{22}H_{15}N_4O_2$	367.1190	5.2	17.5	5	28.0292	C_2H_4
8	349.1090	$C_{22}H_{13}N_4O$	349.1084	1.7	18.5	7	18.0119	H_2O
9	263.1298	$C_{17}H_{15}N_2O$	263.1179	45.2	11.5	[a]		
10	235.1227	$C_{16}H_{15}N_2$	235.1230	−1.3	10.5	5	160.0274	$C_8H_4N_2O_2$ $C_6H_2N_5O$
11	233.0756	$C_{15}H_9N_2O$	233.0709	20.2	12.5	[a]		
12	207.0948	$C_{14}H_{11}N_2$	207.0917	15.0	10.5	10	28.0279	C_2H_4 CH_2N
13	192.0847	$C_{14}H_{10}N$	192.0808	20.3	10.5	12	15.0101	NH

RDB: ring plus double bonds; 0–13: peak numbers shown in Fig. 2.
[a] MS^n study could not be achieved.

Table 4
MS^n fragmentation of the drug.

MS^n	Precursor ion	Product ions
MS^2	611	567, 441, 423
MS^3	567	441, 423
	441	423, 413, 263
MS^4	441	423, 263
	423	395, 380, 263, 235
	413	395, 235
MS^5	423	395, 380
	395	380[a], 367, 349, 235
MS^6	367	349[a], 233
	235	207, 192
MS^7	207	192

[a] Fragments had low intensity, so could not captured for further MS^n.

of *m*/*z* 567 and 441. The ion of *m*/*z* 567 was taken for MS^3 studies, which fragmented into *m*/*z* 441, and further into *m*/*z* 423 and 413. For MS^4 studies, all the above fragments (*m*/*z* 441, 423 and 413) were taken. The MS^n studies were extended up to MS^7 (Table 4). These studies helped in concluding the origin of each fragment and this together with the accurate *m*/*z* values of every fragment helped in outlining the fragmentation pathway, which is described in Fig. 4.

As shown, the major fragment of *m*/*z* 441 was formed on loss of cilexetil moiety ($C_9H_{16}O_3$) from the drug. The ion further fragmented into *m*/*z* 423 with the loss of H_2O molecule. Both these fragments were also formed in an additional pathway from ion of *m*/*z* 567, which itself was formed after removal of ethoxy group from benzimidazole ring of the drug. The other fragments formed are clearly in Fig. 4, along with their corresponding losses.

3.3. LC–MS/TOF studies on stressed samples

To elucidate the structure of each degradation product, all the stressed samples were subjected to LC–MS/TOF analyses. The TOF mass spectra of various degradation products are shown in Fig. 5. The experimental masses, possible molecular formulae and major fragments of degradation products are enlisted in Table 5.

3.4. Postulated structures of degradation products

With the help of major fragments observed in MS/TOF studies and fragmentation pattern of the drug, generalized fragmentation patterns for hydrolytic and photolytic degradation products were outlined, which are described in Figs. 6 and 7, respectively.

3.4.1. DP-I (*m*/*z* 441)

As shown in Fig. 6, five fragments of DP-I (f–j) were similar to the drug. As the drug is composed of candesartan and cilexetil moiety, joined through an ester bond, it could easily be cleaved in basic condition. Hence DP-I was proposed to be the drug devoid of cilexetil moiety.

3.4.2. DP-III (*m*/*z* 583)

The accurate mass difference between drug (*m*/*z* 611.2620) and DP-III (*m*/*z* 583.2307) was 28.0313. This exact mass showed that there was loss of ethyl group (28.0307) instead of N_2 (28.0055), CH_2N (28.0181) or CO (27.9943), the other possibilities with equivalent mass. Further, as shown in Fig. 6, fragments of *m*/*z* 413, 395, 367 and 207 of DP-III were equivalent to fragments e, f, h and j of the drug, respectively. This indicated loss of ethyl group from the benzimidazole ring. A keen observation on the accurate masses of fragments in Tables 3 and 5 revealed that the fragment of *m*/*z* 235.1015 of DP-III was different from equivalent fragment

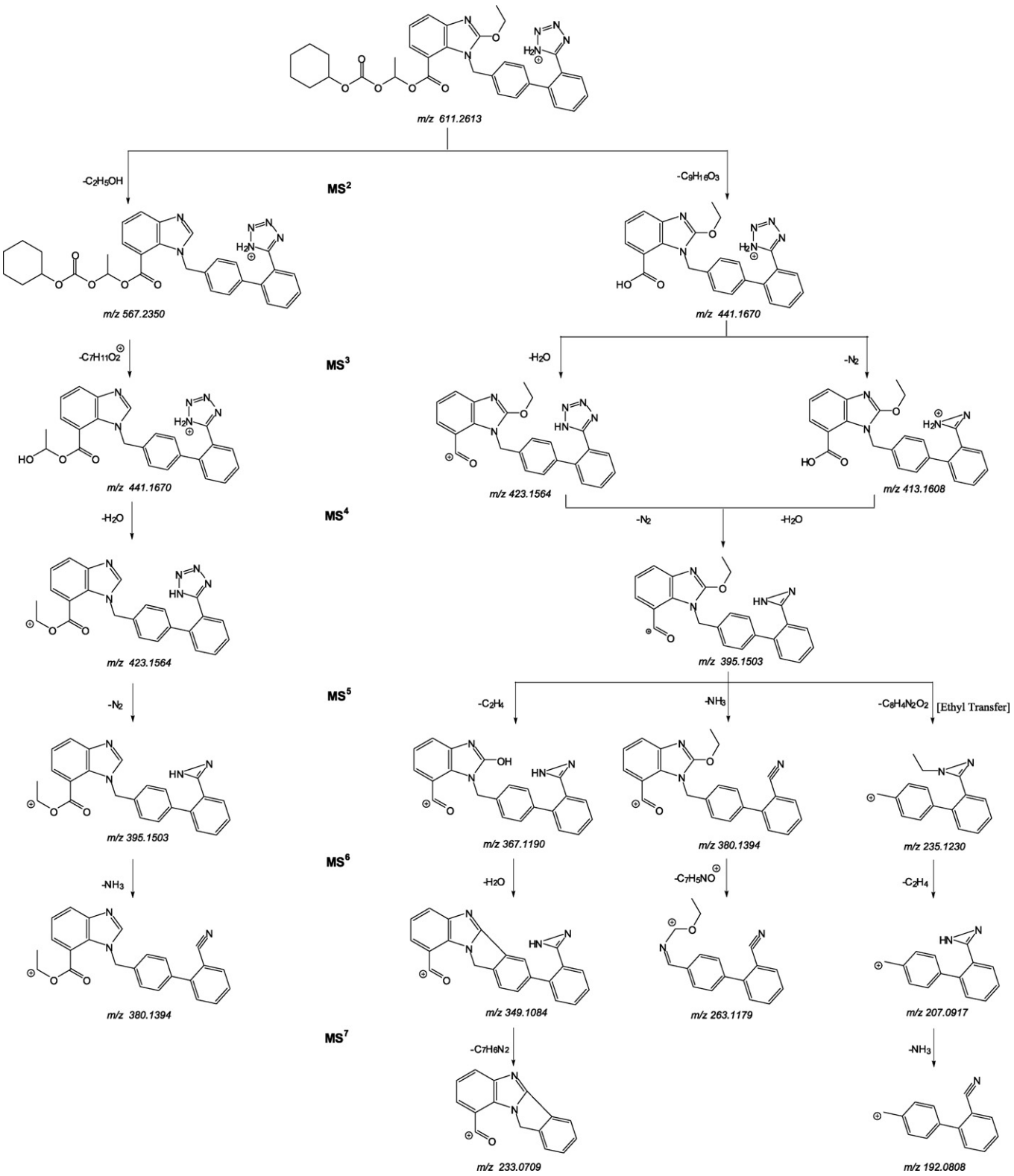

Fig. 4. Fragmentation pathway of the drug along with the exact masses of the fragments.

of drug with *m*/*z* of 235.1227. This indicated that instead of de-ethylated structure of the said fragment of DP-III, the fragment of *m*/*z* 235.1227 in drug was formed by another pathway, logically explained by internal ethyl transfer from the benzimidazole ring (Fig. 4). The same was supported by additional fragment of *m*/*z* 439.1513 in case of DP-III (Fig. 8), which was not possible in the drug.

Further, DP-III was also isolated and subjected to spectral analyses. IR studies did not help in the confirmation of its structure, as there was difference of only an ethyl group between the structures of DP-III and the drug. Fig. 9 shows ^{1}H NMR spectra of the drug and DP-III. In the ^{1}H NMR of DP-III, three hydrogens less than the drug were seen in the region of δ 1.2–1.9. Similarly, the integration of peak at δ 4.6 of DP-III showed the absence of two hydrogens, indicating

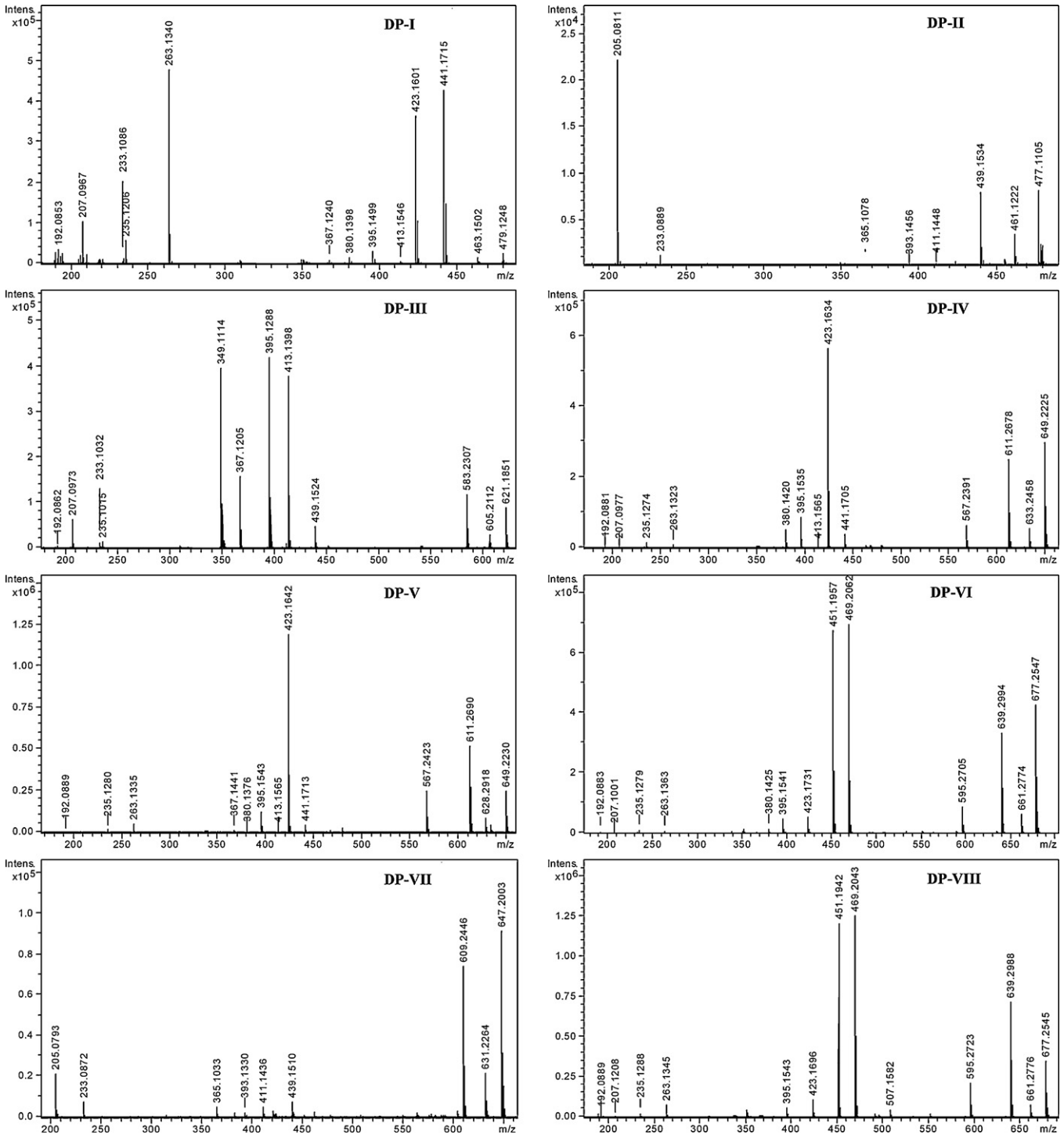

Fig. 5. Line spectra of degradation products DP-I–VIII.

the removal of ethyl group from the drug. For further confirmation of the structure, DEPT 135 was performed on both, drug and DP-III. As shown in Fig. 10, the peak due to CH_3 attached to aliphatic carbon at δ 13.43 and CH_2 peak attached to a hetero atom (oxygen) at δ 67.02 were absent in DP-III.

3.4.3. DP-IV and DP-V (m/z 611)

Both DP-IV (*m*/*z* 611.2678) and DP-V (*m*/*z* 611.2690) had the same high resolution mass as that of the drug (*m*/*z* 611.2620). Moreover, the fragmentation pattern of these was also identical to the drug, which suggested that they were isomeric to each other. For both the degradation products, all the fragments (Fig. 6) could be authenticated with an ethyl group in the tetrazole moiety at *N*1 or *N*2. As the tetrazole compounds are known to exist in annular tautomeric forms (1*H* and 2*H*) [7], therefore, in the neutral condition, ethyl addition could be possible at both *N*1 and *N*2, leading to formation of DP-IV and DP-V. Because both the products had the same fragmentation pattern, it was not possible to distinguish between them merely on the basis of mass studies. Hence, additionally, *c* Log *P* values were determined by ChemDraw Ultra software (version 10) to correlate the retention times on the reversed phase column. *N*1-ethyl had *c* Log *P* value 7.1, which was higher than *N*2-ethyl product

Table 5
MS/TOF data of DPs (I–VIII) along with their experimental masses, possible molecular formula, RDB, theoretical masses, error in ppm and major fragments.

Drug/DPs	Experimental mass	Best possible molecular formulae	RDB	Theoretical mass	Error in ppm	Major fragments (error in ppm, chemical formula)
I	441.1715	$C_{24}H_{21}N_6O_3^+$	17.5	441.1670	10.2	423.1601[a] (8.7), 395.1499[a] (−1.0), 380.1398[a], 367.1240[a] (13.6), 263.1340[a] (61.1), 235.1206[a] (−10.2), 207.0967[a] (24.1), 192.0853[a] (23.4)
II	439.1534	$C_{24}H_{19}N_6O_3^+$	18.5	439.1513	4.8	411.1448 (−0.9, $C_{24}H_{18}N_4O_3^+$), 393.1456 (27.9, $C_{24}H_{17}N_4O_2^+$), 233.0889 (28.7, $C_{14}H_9N_4^+$), 205.0811 (24.8, $C_{14}H_9N_2^+$)
III	583.2307	$C_{31}H_{31}N_6O_6^+$	19.5	583.2300	1.2	439.1524 (2.5, $C_{24}H_{18}N_6O_3^+$), 413.1398[a] (−50.8), 395.1288[a] (−54.4), 367.1205[a](4.0), 349.1114[a] (8.5), 235.1015 (15.7, $C_{14}H_{11}N_4^+$), 207.0973[a] (27.0), 192.0862[a] (28.1)
IV	611.2678	$C_{33}H_{35}N_6O_6^+$	19.5	611.2613	10.6	567.2391[a] (7.2), 441.1705[a] (7.9), 423.1634[a] (18.4), 413.1565[a] (−10.4), 395.1535[a] (8.0), 380.1420[a] (6.8), 235.1274[a] (18.7), 207.0977[a] (28.9), 192.0881[a] (38.0)
V	611.2690	$C_{33}H_{35}N_6O_6^+$	19.5	611.2613	12.6	567.2423[a] (12.8), 441.1713[a] (9.7), 423.1642[a] (18.4), 413.1565[a] (−10.4), 395.1543[a] (10.1), 380.1376[a] (−4.7), 367.1441[a] (68.3), 235.1280[a] (21.2)
VI	639.2994	$C_{35}H_{39}N_6O_6^+$	19.5	639.2926	10.6	595.2705 (7.0, $C_{33}H_{35}N_6O_5^+$), 469.2062 (16.8, $C_{26}H_{25}N_6O_3^+$), 451.1957 (17.7, $C_{26}H_{23}N_6O_2^+$), 423.1731[a] (39.4), 395.1541[a] (9.6), 380.1425[a] (8.1), 207.1001[a] (40.5)
VII	609.2446	$C_{33}H_{33}N_6O_6^+$	19.5	609.2456	−1.6	439.1510 (−0.6, $C_{24}H_{19}N_6O_3^+$), 411.1436 (−3.8, $C_{24}H_{18}N_4O_3^+$), 393.1330 (−4.0, $C_{24}H_{17}N_4O_2^+$), 365.1033 (0.0, $C_{22}H_{13}N_4O_2^+$), 233.0872 (21.4, $C_{14}H_9N_4^+$), 205.0793 (16.0, $C_{14}H_9N_2^+$)
VIII	639.2988	$C_{35}H_{39}N_6O_6^+$	19.5	639.2926	9.7	595.2723 (10.0, $C_{33}H_{35}N_6O_5^+$), 469.2043 (12.7, $C_{26}H_{25}N_6O_3^+$), 451.1942 (14.4, $C_{26}H_{23}N_6O_2^+$), 423.1696[a] (31.1), 395.1543[a] (10.1), 235.1288[a] (24.6), 192.0889[a] (42.1)

[a] The chemical formulae for these *m*/*z* values were the same as given in Table 3 for fragments of equivalent masses of the drug.

(6.9). As shown in the chromatogram in Fig. 1, the resolution of the DP-V and DP-IV was also in the same order. Another observation was that DP-V was formed in higher amount than DP-IV. This was supplemented by a literature reference, according to which the reactivity of 1*H* form of tetrazole predominates over 2*H* form in the solution state [7].

3.4.4. DP-VI and DP-VIII (m/z 639)

Like DP-IV and DP-V, DP-VI and DP-VIII also had same *m*/*z* values and ~28.037 Da higher mass than that of the drug. This propounded addition of an ethyl group to the drug. As shown in Fig. 6, a similar kind of parallelism was observed between DP-IV/DP-V and DP-VI/DP-VIII. The additional ethyl group was proposed again to be

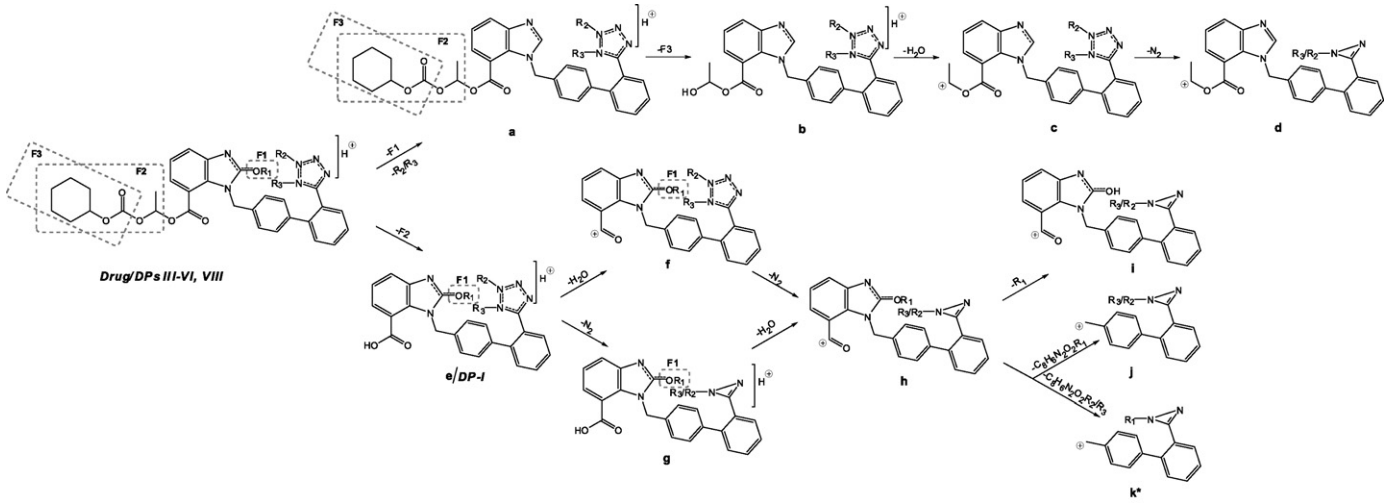

Drug / DPs	R_1	R_2	R_3	Experimental masses										
				a	b	c	d	e	f	g	h	i	j	k*
Drug	C_2H_5	H	-	567	441	423	395	441	423	413	395	367	-	235
I	C_2H_5	H	-	-	-	-	-	-	423	413	395	367	-	235
III	-	H	-	-	-	-	-	413	395	-	367	-	207	-
IV	-	C_2H_5	-	567	441	423	395	441	423	413	395	367	235	-
V	-	-	C_2H_5	567	441	423	395	441	423	413	395	367	235	-
VI	C_2H_5	C_2H_5	-	595	469	451	423	469	451	-	423	395	235	-
VIII	C_2H_5	-	C_2H_5	595	469	451	423	469	451	-	423	395	235	-

Fig. 6. Generalized fragmentation pattern of the drug and its hydrolytic DPs (I, III–VI and VIII) along with their experimental masses. Key: a–k: fragments; R_1-R_3: substitutions; F_1-F_3: common losses; *: For drug and DP-I only.

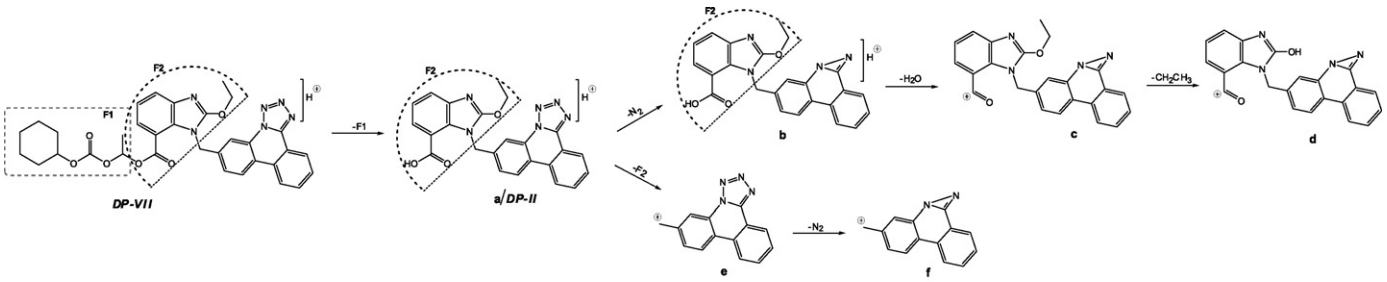

DPs	Experimental masses					
	a	b	c	d	e	f
II	-	411	393	365	233	205
VII	439	411	393	365	233	205

Fig. 7. Generalized fragmentation pattern of the photolytic DPs (II and VII) along with their experimental masses. Key: a–f: fragments; F_1, F_2: common losses.

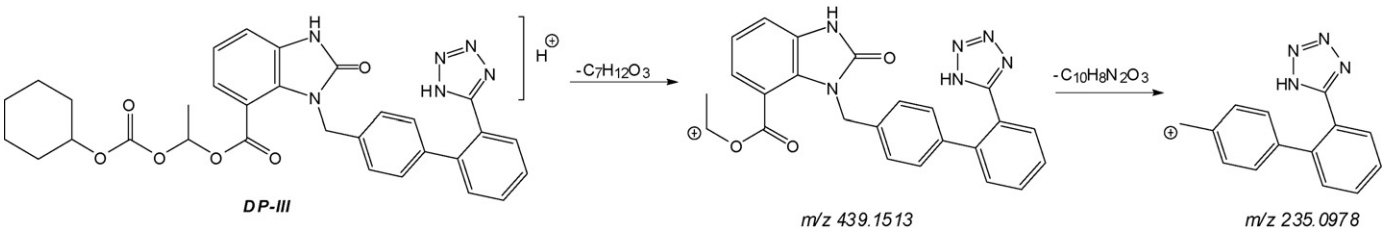

Fig. 8. Additional fragments of DP-III.

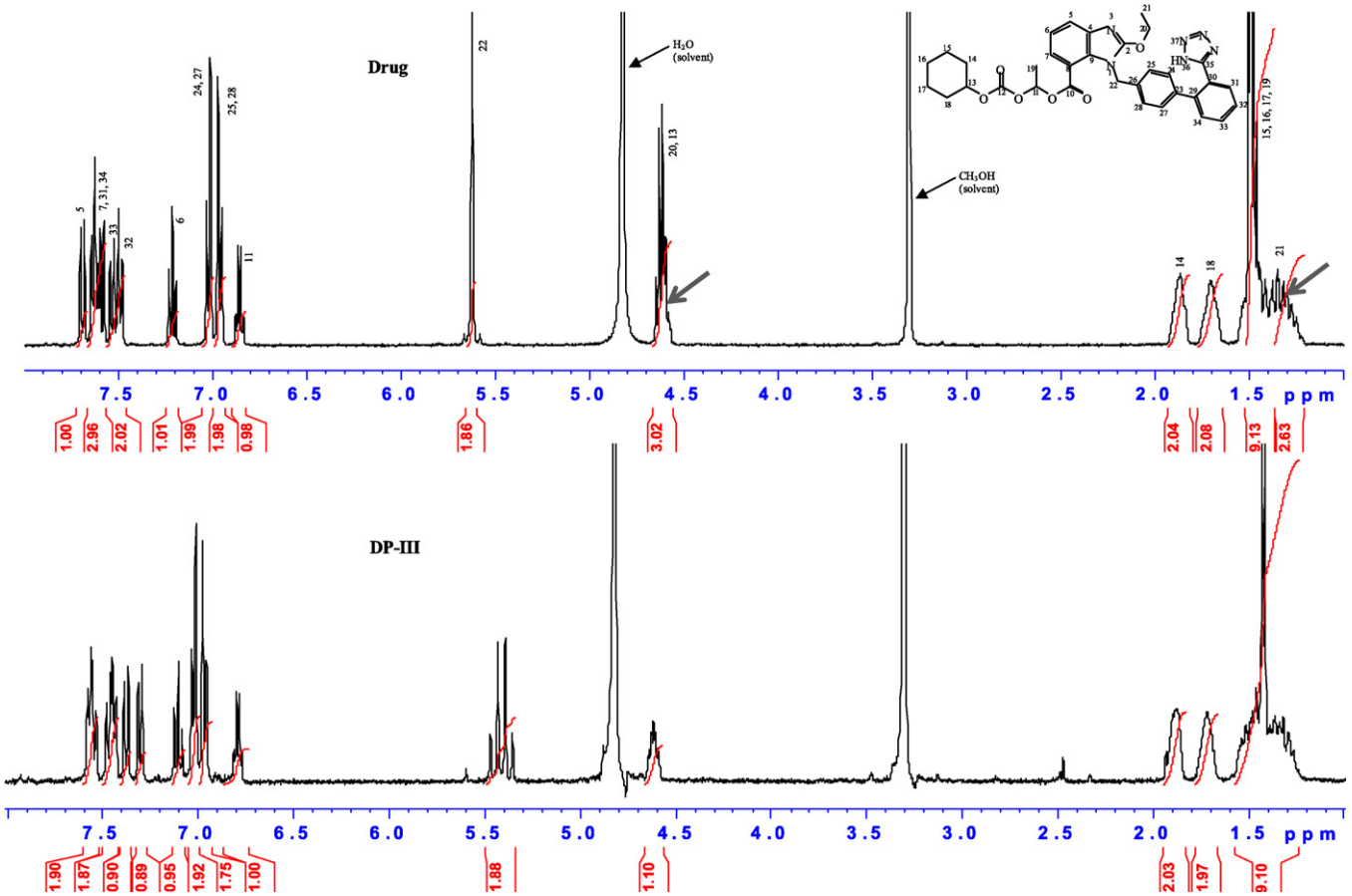

Fig. 9. ^{1}H NMR of the drug and DP-III. Arrows denote the difference in peaks between drug and DP-III.

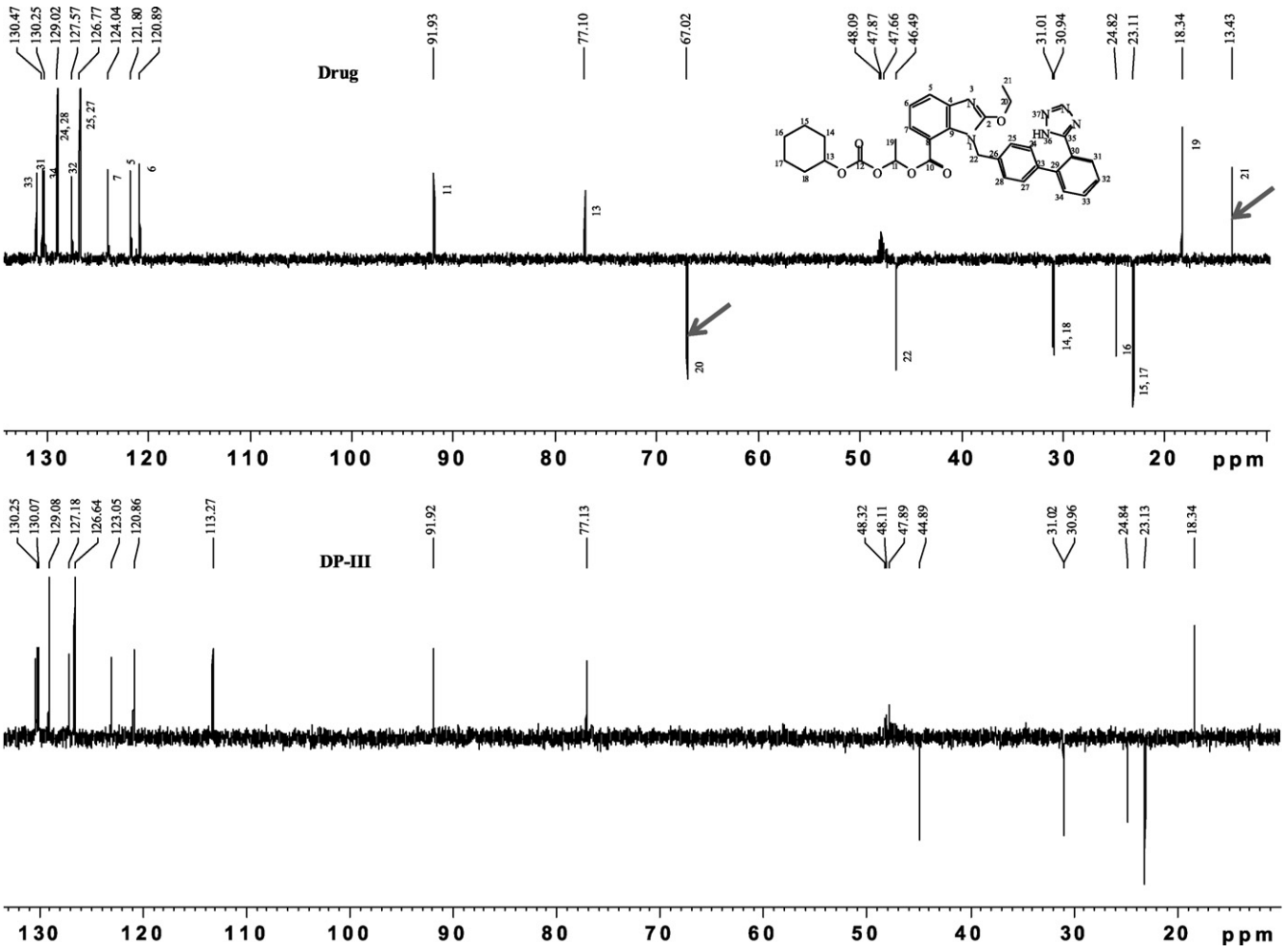

Fig. 10. DEPT 135 of the drug and DP-III. Arrows denote the difference in peaks between drug and DP-III.

present on the tetrazole moiety, similar to that of DP-IV and DP-V, in absence of an alternate site. The two products also had a similar kind of difference in polarity (*N*1-ethyl product; *c* Log *P* 8.1 and *N*2-ethyl product; *c* Log *P* 7.9) as well as the relative extent of formation. Therefore, DP-VI and DP-VIII were proposed to be *N*2-ethyl and *N*1-ethyl derivatives of the drug.

3.4.5. DP-VII and DP-II (m/z 609 and 439)

In MS/TOF studies, DP-VII fragmented into ions of *m*/*z* 439, 411, 393, 365, 233 and 205, each of which was 2 mass units less than the corresponding fragments of the drug (*m*/*z* 441, 413, 395, 367, 235 and 207). Considering this fact, a generalized fragmentation pathway for the photolytic degradation products was outlined, as shown in Fig. 7. From the fragmentation pattern, it was clear that a cyclised product was formed on removal of one hydrogen each from tetrazole and phenyl rings. Such cyclisation phenomenon under photolytic conditions has already been reported in literature [8]. Hence, DP-VII was proposed to be the cyclised analogue of the drug. Under photolytic basic condition, an additional degradation product (DP-II) was formed. This was proposed to be cyclised analogue of DP-I, formed in a similar way to the formation of DP-VII from the drug.

3.5. Postulated degradation pathway of the drug

The drug readily underwent ester hydrolysis under basic condition to form DP-I with the removal of cilexetil moiety. Under photolytic conditions, the cyclisation of the drug resulted in the formation of DP-VII. Like DP-I, DP-VII also underwent ester hydrolysis in the basic condition, to form DP-II. The latter was also directly formed from DP-I under photolytic basic conditions through cyclisation. DP-III was formed in both neutral and acidic conditions through hydrolysis of ether bond between benzimidazole and ethyl moiety. The leaving ethyl group was attacked by *N*2 or *N*1 of tetrazole ring of DP-III to form DP-IV and DP-V. Similarly, DP-VI and DP-VIII were formed by ethylation on tetrazole moeity. The schematic representation of the degradation pathway is shown in Fig. 11.

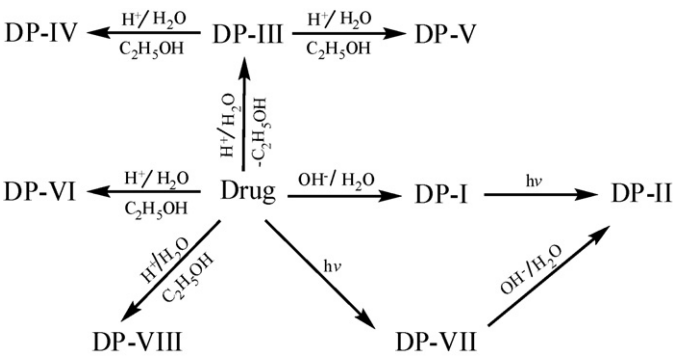

Fig. 11. Degradation pathway of the drug.

3.6. Explanation to the observed degradation behaviour

The maximum numbers of degradation products were formed in neutral rather than acidic/basic conditions. The reason may be that under basic conditions, the cilexetil part was very rapidly removed from the drug, so that other DPs, which were isomeric to the drug, could not be formed. Under acidic condition, only DP-III was formed and whole of the drug was decomposed on prolonged heating. Hence, it clearly excluded the formation of DP-VI and DP-VIII, which could be produced only after ethylation of the drug. DP-IV and DP-V could be formed in the presence of DP-III but this did not occur. This may be attributed to the fact that under acidic conditions, protonation of tetrazole moiety occurred by utilizing the lone pair of electrons of *N*1 or *N*2, and this did not leave any room for ethylation at those positions.

4. Conclusions

Stress degradation studies on candesartan cilexetil, carried out according to ICH guidelines, provided information regarding degradation behaviour of the drug under various conditions of hydrolysis, oxidation, photolysis and thermal conditions. HPLC analyses revealed formation of eight degradation products, in total. All the products were characterized with the help of LC–MS/TOF studies. It was found that four of the degradation products were hitherto unknown. Hence, a more comprehensive degradation pathway of the drug was outlined. Also a complete fragmentation pathway of the drug was established, which is not known earlier. The latter may be useful in future investigations on characterization of process related impurities, drug–excipient interaction products, and metabolites of the drug using LC–MS techniques.

References

[1] C.H. Gleiter, C. Jagle, U. Gresser, K. Morike, Cardiovasc. Drug Rev. 22 (2004) 263–284.
[2] N. Ferreirós, S. Dresen, R.M. Alonso, W. Weinmann, J. Chromatogr. B 855 (2007) 134–138.
[3] D.V. Subba Rao, P. Radhakrishnanand, M.V. Suryanarayana, V. Himabindu, Chromatographia 66 (2007) 499–507.
[4] ICH Q1B, International Conference on Harmonisation, IFMPA, Geneva, 1996.
[5] ICH Q1A (R2), International Conference on Harmonisation, IFMPA, Geneva, 2003.
[6] S. Singh, M. Bakshi, Pharm. Technol. On-line 24 (2000) 1–14.
[7] T. Eicher, S. Hauptmann, A. Speicher, The Chemistry of Heterocycles Structure, Reactions, Syntheses and Applications, Wiley-VCH GmbH and Co. KGaA, Weinheim, 2003, pp. 213–214.
[8] R.P. Shah, V. Kumar, S. Singh, Rapid Commun. Mass Spectrom. 22 (2008) 613–622.